The Performance Analysis for the New Architecture of DWDM Network

Dong Sun Lee* *Regular Member*

ABSTRACT

Aggregate bandwidth required by the internet is expected to be explosively increased. To meet this anticipated need, an ultra high speed internet backbone transport network, capable of supporting up to a Tbps traffic capacity, is required. this thesis examines, through computer simulation and modeling, the technological requirements and assesses the performance analysis and feasibility for implementing ultra-high speed NGI backbone transport network fabric based on WDM technology. The study results are that C/L band EDFA spectral gains for ultra high speed DWDM have been improved from 2.61dB/1.5386dB to 0.03dB/0.096dB by proposed architecture.

Key Words : WDM, NGI, EDFA, WADM, GEF, FBG

Ⅰ. Introduction

WDM(Wavelength-Division Multiplexing) technology has emerged as the leading solution high-speed transmission application and has been the demanding technology of next generation networks. Aggregate bandwidth required by the internet is expected to be explosively increased. To meet this anticipated need, an ultra high speed internet backbone transport network, capable of supporting up to a Tbps traffic capacity, is required. Specifically, this thesis examines, through computer simulation and modeling, the technological requirements and assesses the performance analysis and feasibility for implementing ultra-high speed NGI (Next- Generation Internet) backbone transport network fabric based on WDM technology. Our study evaluates the end-to-end performance of a ring- based topology backbone transport network.

A ring topology has been selected here for two main reasons: 1) It is considered as a powerful candidate for introducing DWDM into the access environment due to its inherent reliability[1][2][3]. And 2) A mesh-based backbone transport network topology can be partitioned into several smaller inter-connected rings. Thus, a ring topology will constitute fundamental building block for NGI backbone transport network facilities.

Ⅱ. Key Technological Requirements

Two key technological issues need to be addressed before the successful implementation of the proposed ultra-high speed NGI backbone WDM transport network fabric:

A. Novel architectures that offer a possible route to ultra-broad band amplifiers capable of providing 60-80nm of optical bandwidth based on erbium-doped silica fiber must be developed. Using these ultra-broad band ESFAs, the number of WDM channels can then grow to about 80-100 channels while keeping a channel spacing compatible with practical filtering technology.

One possible solution for broad-band EDFAs is achieved using new materials. Erbium-doped fluoride fibers have been shown to provide a gain bandwidth of 24nm without GEF.

* 광운대학교 정보제어공학과 (dsleekorea@hanmail.net)
논문번호 : KICS2007-07-307, 접수일자 : 2007년 7월 11일, 최종논문접수일자 : 2008년 5월 29일

Erbium-doped tellurite fibers have also been reported to be a promising candidate. However, the gain spectrum of tellurite EDF is highly non-uniform and many other properties need to be investigated before such fibers can be qualified for practical applications. Alternatively, new architectures offer a possible route to broad band amplifiers based on erbium-doped silica fiber. Previous work has shown that optical gain can be obtained in erbium-doped silica fibers in the long wavelength range between 1570 and 1600nm (called L-band here).

This thesis examines and develops a novel two-band EDFA configuration capable of providing as large as 80nm of optical bandwidth using only silica-based EDFAs. This is achieved by combining the gain in the conventional wavelength range between 1525 and 1565nm(called C-band in this thesis) and that in the long wavelength range between 1570 and 1610nm(called L-band here). Each configuration consists of two parallel dual-stage silica-based EDFA, where each dual-stage is independently optimized. Such configurations offer a practical route to remove the bandwidth limitation which currently constrains the design of flexible WDM systems and networks. With 80nm of bandwidth, this EDFA configuration will be able to accommodate 100 WDM channels with the ITU standard channel spacing of 100GHz.

Specifically, this thesis investigates and develops ultra wide-band gain-flattened and stabilized silica-based ESFA configuration with flexible and scalable WADM capabilities. The WADM is assumed to be located between the dual-stage EDFA of each band. Each WADM consists of short-period fiber grating filters along with circulators and a given number of wavelength selective elements depending on the number of wavelengths to be added/dropped, to perform the WADM capabilities. These configurations must be capable of satisfying the following:

- Low-noise and high output power.
- Gain flatness should be independent of the operating conditions(signal and pump power levels, etc.).
- Maintain constant per-channel output power with a minimally degraded SNR, regardless of the number of channels present, over a wide dynamic range of input signal levels.
- Amplify and add/drop any number of wavelengths ranging from one to perhaps 25 depending on the wavelength assignment plan.
- Flexible for graceful in-service upgrade to maximum of 100 WDM channels along with the smooth evolution in increasing the bit rate per channel from OC-12 to OC-192.

B. A novel practical filtering technology that is compatible with the channel spacing must also be developed and investigated. Specifically, this work examines novel WDM switching technologies using long/short period fiber grating filters. The feasibility of using one new feature, crucial for broadband long-haul WDM transmission systems, to equalize (flatten) the passband of cascaded EDFAs will be examined Long-period fiber gratings will be used to flatten the gain and broaden the optical bandwidth of a two-stage mid-amplifier pumped EDFAs.

2.1 Two-Band EDFA Architecture

Figure 1 shows an architecture of the proposed two-band EDFA configuration. It consists of two parallel dual-stage silica-based EDFA, where each dual-stage is independently optimized first for output power and secondly for gain flatness over the 40nm signals bandwidth.

Circulators and broad FBG(Fiber Bragg Grating) that reflect the C-band are used to demultiplex and multiplex the two bands before and after amplification, respectively. Thus, the two bands are amplified separately and are recombined afterwards. The circulators also act as an isolator. Both bands use the same type of silica-based fibers but with longer amplifier lengths for the L-band.

2.2 WADM Architecture

A WADM is assumed to be located between the dual-stage EDFA of each band, as shown in Figure 1. Each WADM, as shown in Figure 2, consists of short-period fiber grating filters along with circulators and a given number of wavelength selective elements depending on the number of wavelengths to be added/dropped at a given node, to perform the WADM capabilities.

For a fixed WADM configuration, the number of short-period grating filters will depend on the wavelength drop/add assignment plan. However, for a fully reconfigurable WADM, the number of short-period grating filters should equal the total number of wavelengths passing through the EDFA configuration. This study will examine two techniques to investigate the potential and the feasibility of programmable and/or tunable short-period grating filters in the following paragraphs. Another critical criterion that must be met in the design

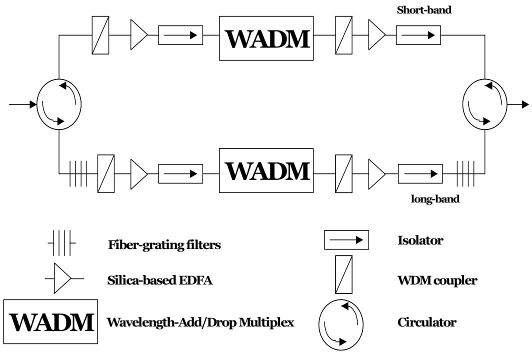

Fig. 1. The schematic diagram of one architecture of proposed dual-band EDFA Config

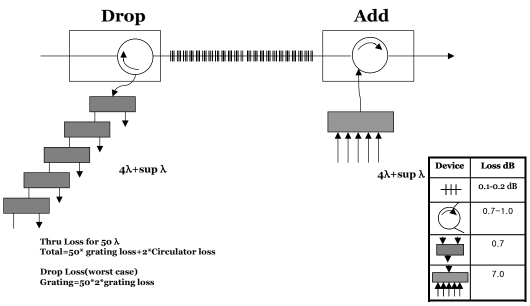

Fig. 2. The fixed add/drop method

of our proposed EDFA configuration in its flexibility for graceful in-service upgrade to a maximum of 100 WDM channels along with the smooth evolution in increasing the bit rate per channel from OC-12 to OC-192.

There are two type building blocks of WADM: the S-type building block and bragg wavelength tuning building block[4]. Figure 3 shows the series type of building block. The series of FBG elements and 2×2 optical switches are used with each FBG inserted between two 2×2 optical switches, each optical switch has one of the "cross" and the "bar" operation stated at one time. Switching two 2×2 optical switch's, one in front of and one after the FBG element, to the "cross" state, the passed through channel signal will be reflected by the connected FBG element, then leaving from the dropped port of circulators. In the mean time, other crossed-connected channel signals can be spatially passed through the FBG chain to another fiber link. When two or more 2×2 optical switches are properly arranged in the S-type building block, multiple channel adding/dropping can then be realized. Figure 3(b) illustrated that the wavelengths λ1 and λ2 are simultaneously reflected and thus passed-though the 2×2 WXC when the first and the third optical switched are in the "cross" states and other optical switches are in the "bar" stated. For rearrangeable add/drop operation, the number of required 2×2 optical switches, $U = m + 1$, and total number of required

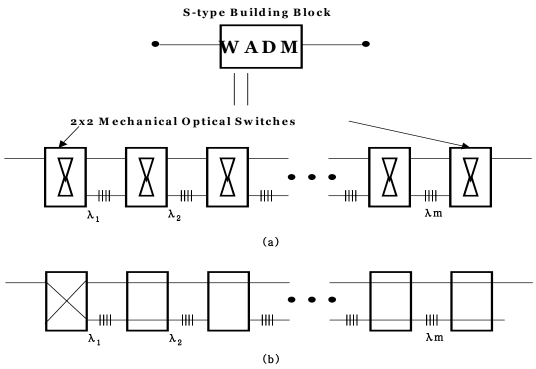

Fig. 3. S-type building block (a) the schematic diagram of the series S-type building block "FGR" (b) its operating principle

FBG's, Q=m, respectively. Here m refers to total number of wavelengths passing Add/Drop module. The feasibility of the S-type building block has been probed.

Figure 4 shows the nonswitched voltage-controlled building block, in which a series of FBG's with appropriate control devices are used but with no more optical switches. The voltage-controlled narrow band fiber gratings with high reflectivity to the targeted wavelengths and low transmission loss for other bypassing wavelengths are used to cooperate the circulators to implement the add and drop functionality. Here WADM consists of FBG filters to provide low cross-talk performance, and no signal degradation is occurred. The FWHM(i.e., 3dB passband width) of each FBG should be large enough to cover the corresponding channel signal with high reflectivity and low out-of-band transmission loss.

The voltage controllers are used to control the reflected FBG window's position to selectively choose the added or dropped wavelengths. The voltage-driven PZT(Piezoelectrical Transducer) devices or the stepping motors can be used to implement the central wavelength-shift control each FBG by using compressive stress on the FBG. In predecessor's experiment, the wavelength tuning rage can achieve ±50nm, and a wavelength resolution of ±2pm. When the voltage is released, the bragg fiber grating windows(in Figure 4 (b)) will be in OFF status, and when the voltage is supplied, the spectra windows shift to the desired position, this status is considered as ON. The voltage-controlled fiber grating has two states: ON and OFF. In OFF status, the grating window will locate at the dropped wavelength, both signal and ASE at that wavelength get reflected to drop port through circulator without passing to next EDFA. In ON status, the signal at wavelength λ will be passed, the voltage-controlled grating window will shift 0.4nm(the half of the channel spacing) to right, so that ASE at λ+0.4nm will be disappeared from the next EDFA. This design can significantly reduce the ASE accumulation and improve the SNR. For the add wavelengths, they are added through the add port of circulator, reflected by WADM, and fed into WDM system through another arm of circulator. Compared with the S-type building block, the bragg wavelength tuning building block can reduce the insertion loss, which is caused by the optical switches, and increase the optical SNR. Therefore in out node structure, the bragg tuning building block is used.

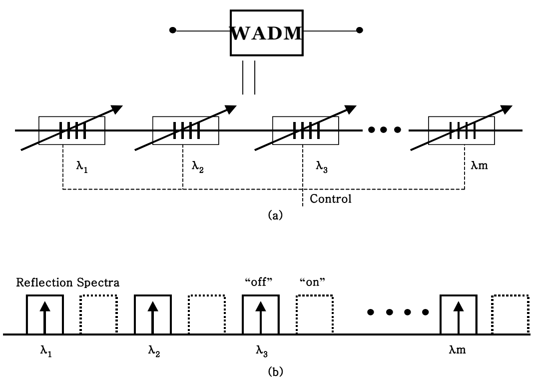

Fig. 4. The nonswitched voltage-controlled building block (a) the schematic diagram of the FGR block (b) its operation principle

2.3 Gain Equalization

Since the amplification of a WDM signal by non-equalized EDFAs may result in signal distortion and poor signal to noise ratio performances, several methods, either intrinsic or extrinsic, have been proposed to equalize the gain of EDFAs. Intrinsic methods consist of modifying the spectroscopic properties of erbium ions by a change in codoping ions or glass matrix. Alumino-silicate[5] or fluoride-based[6] glasses are such host matrixes that improve the flatness of EDFA gain spectra. However, intrinsically equalized amplifiers are accurate over a limited bandwidth. Extrinsic methods equalize the gain by making use of a filtering device connected in series with the EDFA. In-fiber filters that have been previously demonstrated include acoustooptic tunable filters[7], long-period gratings[8] or blazed gratings[9]. The main limitation of an acoustooptic filter is its high RF power consumption. Long-period and blazed gratings are sensitive to environmental conditions since they rely on coupling from guided to nonguided modes.

Table 1. The configuration parameter setting of each EDFA in figure 3-8

PARAMETER	EDFA1 (C-band)	EDFA2 (C-band)	EDFA3 (L-band)	EDFA4 (L-band)
Input power per Channel (dBm)	-15	-14	-15	-14
Forward Pump power (mW)@980nm	78	60.5	185	68.5
Amplifier length(m)	8.8	4.8	74	51

Furthermore, their manufacturing complexity rapidly increases when the equalization bandwidth is extended. The predecessor have shown that bragg gratings placed after each amplification stage can equalize the gain of cascaded EDFAs. However, each of the narrow-band filters used was attenuating a single channel and therefore most of the ASE (Amplified Spontaneous Emission) was transmitted. This study uses gain equalization performed using various configurations of spectrally designed bragg gratings in the front of the latter stage amplifier.

Long-period fiber gratings will be used to flatten the gain and broaden the optical bandwidth of EDFAs. The ideal FBG filter spectrum is computed based on the following optimization method.

A. For given total input power, $P_{in}^{(2)}$ At the input of the second stage EDFA, determine the intrinsic WDM gain spectra. $G_{intrinsic}(\lambda)$.

B. Determine the input signal level/channel $P_{in,flat}^{(2)}$ (λ), required to produce a at output spectrum over the desired signals at the output of the second stage by first using the normalized WDM signal gain spectra, $G_{normalized}(\lambda)$, defined as

$G_{normalized}(\lambda)=G_L/G_{intrinsic}(\lambda)$, then

$$P_{in,flat}^{(2)}(\lambda)=G_{normalized}(\lambda)*P_{in}^{(2)}/\sum_{\lambda} G_{normalized}(\lambda)$$

Where G_L Is the least-favored signal gain from among all of the signal wavelengths and $P_{in}^{(2)}=\sum_{\lambda} P_{in,flat}^{(2)}(\lambda)$

C. Determine the first stage EDFA output spectra, $P_{out}^{(1)}(\lambda)$.

D. Determine the transmission characteristic of the long period fiber grating, $T(\lambda)$, by using $P_{out}^{(1)}(\lambda)$*(total intra-stage loss)*$T(\lambda)=P_{in,flat}^{(2)}(\lambda)$

Ⅲ. The System Model

The ultra-high speed DWDM-based ring network under consideration consists of 24 nodes. Successive nodes are separated by fiber loss of 10 dB, which corresponds to 40km × 0.25 dB/km. Seventy-eight wavelengths are needed to achieve full-mesh connectivity between 24 nodes, and 12 wavelengths are added/dropped at each node. The schematic diagram of the node structure is shown in Figure 5.

The system model consists of 78 WDM channels subdivided into two subbands, the C-band and the L-band. 33-channels are spaced 100GHz apart in the 1537.4(channel 1) to 1563.8nm (channel 33) amplifier C-band and the remaining 45-channels are also spaced 100GHz apart in the 1572.6 (channel 34) to 1608.6nm(channel 78) amplifier L-band. Circulators and broad band FBG that reflect the C-band are used to demultiplex and multiplex the two bands before and after amplification, respectively. Thus, the two bands are amplified separately and are recombined afterwards. Both bands use the same type of silica-based fibers but with longer amplifier lengths for the L-band.

The two-band EDFA configuration, shown in Figure 5, consists of two parallel dual-state silica-based EDFA, where each dual-stage is independently optimized first for output power and secondly for gain flatness over the desired signals bandwidth. The C-band dual-stage EDFA used in

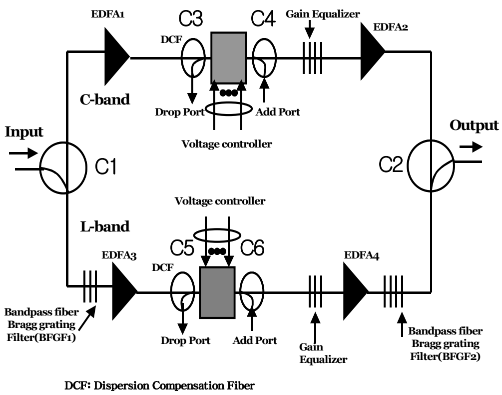

Fig. 5. Proposed node architecture by adopting WDM and FBG technologies

the simulation is co-pumped with 78 mW of pump power at 980nm in stage 1 and with 60.5 nW at 980nm in stage 2. The L-band dual-stage EDFA is co-pumped with 185 mW of pump power in stage 1 and with 68.5 mW of pump power in the forward direction in stage 2(see Table 1). The design of both amplifier stages for each band was chosen to produce an average dual-stage net gain of about 13 dB.

The alumino-germano silicate EDFA used in the simulation is a commercially available fiber designed for high output power. A long-period fiber grating filter gain equalizer is located between the stages of both the C and L arms along with an isolator and a DCF.

Ⅳ. Simulation and Result Discussion

The ring transmission fiber consisted of twenty-four 40 km spans of standard SMF having an average chromatic dispersion of +17 ps/km-nm and an average attenuation of 0.25 dB/km. Each span is followed by 5.667 km of DCF, located between the dual-stage EDFA of each band, having an average chromatic dispersion of -120 ps/km-nm and an average attenuation of 0.45 dB/km. The average dual-stage net gain of 13 dB is set equal the sum of the span loss between successive nodes 40 km × 0.25 dB/km=10 dB, and the 3dB input/output coupling loss.

The signal and ASE power accumulation along the EDFA chain is determined based on the spectrally resolved numerical model. The accumulated optical SNR(signal-to-noise ratio) reported here is the ratio between the signal level and the accumulated ASE noise power in a 0.2nm optical bandwidth. The end-to-end system performance is estimated from the optical SNR, which must be more than 18 dB(0.2nm resolution) to achieve a bit-error rate of 10~14 at 10 Gbps. Figure 6 and Figure 7 show calculation of the output signal levels and the ASE power in a 0.2nm optical bandwidth for both the C and L band, with and without gain equalization, respectively.

As can be seen from Figure 6, the intrinsic C-band dual-stage EDFA spectral gain variation of 2.61 dB ($G_{max}(\lambda)$=13.09 dB, $G_{min}(\lambda)$=10.48 dB) over 26.4nm bandwidth is reduced to less than 0.03 dB ($G_{max}(\lambda)$=12.0268 dB, $G_{min}(\lambda)$=12.00 dB). It can also be seen from Figure 7 that the intrinsic L-band dual-stage EDFA spectral gain variation of 1.5386 dB ($G_{max}(\lambda)$=12.6186 dB, $G_{min}(\lambda)$=11.08 dB) over 36nm bandwidth is reduced to less than 0.096 dB ($G_{max}(\lambda)$=12.046 dB, $G_{min}(\lambda)$=11.95 dB).

Figure 8 and 9 show the output signal and SNR at node 21. Node 21 was chosen because it corresponds to the worst case performance scenario among 24 nodes. The worst-case channels perform in this node are the C-band channel 3(λ3=1539.0nm) and the L-band channel 67(λ67=1598.0nm). Note that λ3 traverses 9 node while λ67 traverses 12 nodes.

As can be seen from Figure 8 and Figure 9, although the output signal levels are almost the

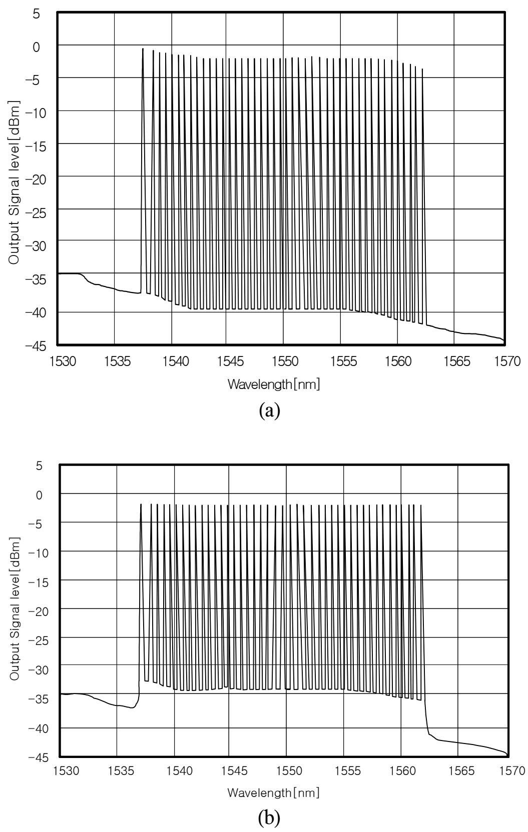

Fig. 6. The output of C band EDFA2
(a) without gain equalizer (b) with gain equalizer

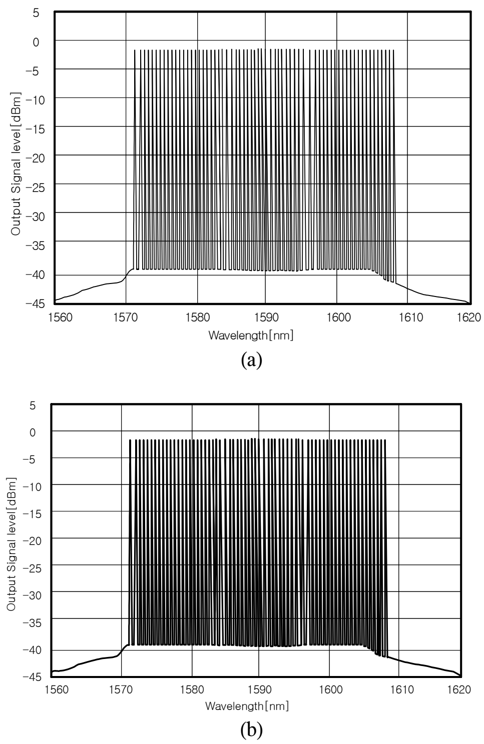

Fig. 7. The output of L band EDFA4
(a) without gain equalizer (b) with gain equalizer

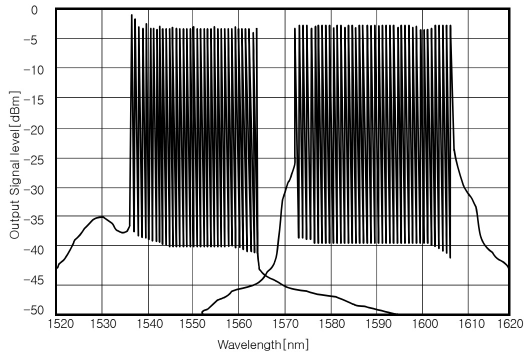

Fig. 8. The output spectra of node 21 pre-EDFA

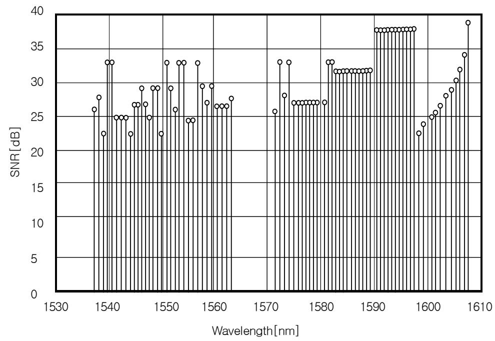

Fig. 9. The SNR of signals from node 21 pre-EDFA

same, however, the SNR is drastically different for each channel. Note, however the worst SNR value at channel 3 (23.15 dB) is still adequate for 10 Gbps operation.

Ⅴ. Conclusion

To meet an explosive demand, an ultra high speed internet backbone transport network, capable of supporting up to a Tbps traffic capacity, is required. This thesis has examined, through computer simulation and modeling, the new technological requirements and has assessed the performance analysis and feasibility for implementing a dynamic and scalable ultra-high speed transport network fabric based on SHR network topology and DWDM technology. The simulation results of a proposed methode have shown an improved performance. The study results are that C/L band EDFA spectral gains for ultra high speed DWDM have been improved from 2.61dB/1.5386dB to 0.03dB/0.096dB by proposed architecture.

References

〔1〕 Jane M Simmons and Adel Saleh, “Optical Regional Access Network (Oran) Project,” OFC ’99, Paper WK1-1, 1999.

〔2〕 F. Elrefaie, “Multi-Wavelength Survivable Ring Network Architectures”, ICC ’93, Paper48, pp. 23-26, May 1993.

〔3〕 M.Rochette, “Gain Equalization of Edfas with Brag Gratings”, IEEE Phostonics Technology Letters, May 1999.

〔4〕 Yung-Kuang Chen, Chien-Chung Lee, “Fiber Bragg Grating- Based Large Non-Blocking Multiwavelength Cross- Connects”, J. Lightwave Technology, Vol.16, pp.1746-1756, Oct. 1998.

〔5〕 T. Terahara, T. Naito, N. Shimojob, T. Tanaka, T. Chikama, and M. Suyama, “0.7Tbps (66× 10.66 Gbps) WDM Transmission Over 2,212 Km using Broadband, High-Power EDFAs with Pump Reflector”, Electron. Lett., Vol.34, No.10, pp.1001-1002, 1998.

〔6〕 M. Yamada, O. Hirotaka, T. Kanamori, T. Sakamoto, Y. Ohishi, And S. Sudo, “A Low

Noise and Gain-Flattened Amplifier Composed of a Silica-Based and a Fluoride-Based Er3+ Doped Fiber Amplifier in a Cascade Configuration", IEEE Photon. Technology Lett., Vol.8, pp.620-622, May 1996.
〔7〕 H. S. Kim, S. H. Yun, H. K. Kim, N. Park, and B. Y. Kim, "Actively Gain-Flattened Erbium-Doped Fiber Amplifier over 35 nm by using All-Fiber Acoustooptic Tunable Filters", IEEE Photon. Technol Lett., Vol.10, pp.790-792, June 1998.
〔8〕 Y. Sun, J. B. Judkins, A. K. Strivastava, L. Garett, J. L. Zyskind, 3. W. Sulhoff, C. Wolf, R. M. Derosier, A. H. Gnauck, R. W. Tkaeh, J. Zhou, R. P. Espindola, A. M. Vengsarkar, and A. R. Chraplyvy, "Transmission of 32-WDM 10-Gbps Channels Over 640 Km using Broad-Band, Gain-Flattened Erbium-Doped Silica Fiber Amplifiers", IEEE Photon. Technology Lett., Vol.9, pp.1652-1654, Dec. 1997.
〔9〕 R. Kashyap, R. Wyatt, and P. F. Mckee, "Wavelength Flattened Saturated Erbium Amplifier using Multiple Side-Tap Bragg Gratings", Electron. Lett., Vol. 29, No.11, pp.1025-1026, 1993.
〔10〕 O. Gautoeron, P. Sansonetti, G. Bassier, and I. Riant, "Optical Gain Equalization with Short Period Fiber Gratings", In Tech. Dig. ECOC'9., Edinburgh, Scotland, U.K., 1997.
〔11〕 A. R. Giles and E. Desurvire, "Modeling Erbium-Doped Fiber Amplifiers", J. Lightwave Technology, Vol. 9, pp.271-283, 1991.
〔12〕 Dietrich Marcuse, "Derivation of Analytical Expressions for the Bit-Error Probability in Lightwave Systems with Optical Amplifiers", J. Lighwave Technology, Vol.8, No.12, pp.1816-1823, 1990.
〔13〕 J. Pan, M. A. Ali, A. Elrefaie, and R. Wagner, "Multiwavelength Fiber Amplifier Cascades with Equalization Employing Mach-Zehnder Optical Filter", IEEE Photon. Lett., Vol.7, pp.1501-1503, Dec. 1995.
〔14〕 Ezhan Karasan, and Ender Ayanoglu, "Performance of WDM Transport Networks", IEEE Journal on Selected Areas in Communications, Vol.16, No.7. Sep. 1998.

이 동 선 (Dong Sun Lee) 정회원
1984년 2월 광운대학교 공대 전기공학과(공학사)
1987년 8월 광운대학원 전기공학과(공학석사)
2004년 8월 광운대학원 정보제어공학과(공학박사)
현재 SNS네트웍스 / 대표이사
<관심분야> 광통신공학, WDM, 광무선신호